Spatial-confinement effect on phonons and excitons in PbI_2 microcrystallites

Shingo Saito* and Takenari Goto
Department of Physics, Faculty of Science, Tohoku University, Sendai 980-77, Japan
(Received 29 March 1995)

We have measured resonant Raman spectra and exciton absorption spectra of PbI_2 microcrystallites embedded in ethylene metacrylic acid (E-MAA) copolymer at 77 and 2 K, respectively. The microcrystallites are plateletlike and vary in thickness. In the resonant Raman spectra, a new line is observed in the acoustic-phonon energy region, which is intimately related to the exciton absorption band in the ultrathin microcrystallite with finite number of layers. The phonon energy as a function of the crystal thickness is explained on the basis of a finite chain model. From this analysis, the relationship between the exciton absorption band and the number of layers is confirmed. Using this relation, we reinterpret the dependence of the exciton energy on the layer thickness, which has been measured previously. Consequently, the thickness dependence of the exciton energy is well explained by the quantum confinement model of the exciton translational motion in the crystallites with more than five layers. In crystallites with thinner layers, however, the exciton energies deviate from the theoretical values.

I. INTRODUCTION

Electronic properties in low-dimensional semiconductors, such as quantum wells, wires, and dots, have been studied by various methods.[1] With the development of sample preparation methods in recent years, electron confinement in a quasi-two-dimensional system has been studied using thin films of GaAs (Ref. 2) and CdTe (Ref. 3) and ultrathin films of CuCl.[4] Exciton polariton interference has been reported in Refs. 2 and 3, and the confinement of translation motion of excitons in Ref. 4. In addition to these materials, ultrathin films of layered semiconductors, such as MoS_2,[5] WSe_2,[6] and PbI_2,[7-9] have been utilized for studying the optical properties of quantum confinement. PbI_2 crystal is one of the typical layered semiconductors.

The lead and iodine atoms within a layer are strongly bonded. Layers are repeated in units of I-Pb-I in the c direction and are bonded to each other by van der Waals forces. There exist many polytypes which differ in the way in which layers are stacked, because of weak interlayer bonding. For example, the crystal structure of the $2H$ polytype belongs to the space group D_{3d}^3 and that of the $4H$ polytype to C_{6V}^4. In the absorption spectrum of the bulk crystal, three narrow bands, probably due to an exciton, were observed by Tubbs.[10] The electronic structure of the $2H$ polytype was calculated by Doni, Grosso, and Spavieri using a semiempirical tight-binding method,[11] by Schlüter and Schlüter using an empirical pseudopotential method,[12] and by Bordas, Robertson, and Jakobsson using a linear combination of atomic orbitals method.[13] According to Schlüter and Schlüter's paper, the smallest band gap appears at point A of the Brillouin zone. The lowest conduction band at point A is split into three bands by the crystal field and the spin-orbit interaction. From group-theoretical analysis, transitions from the top of the valence band to the three conduction bands are represented in symmetry by $A_4^+ \rightarrow A_4^-$, $A_4^+ \rightarrow A_{5,6}^-$, and $A_4^+ \rightarrow A_4^-$, in order of increasing energy. It is assumed that excitons associated with these three transitions correspond to the observed narrow absorption bands. In 1989, Nagamune, Takeyama, and Mirua[14] measured diagmagnetic energy shifts of the band-edge exciton series under strong magnetic field and concluded that the exciton binding energy is about 30 meV.

The translational mass of the exciton in the c direction has been measured as $(1.0\pm0.2)m_0$ by Hayashi[15] from the interference spectrum of the exciton polariton. The electron masses parallel and perpendicular to the c axis are obtained as $m_{e\parallel}=2.1m_0$ and $m_{e\perp}=0.48m_0$, respectively, by Goto,[16] and the isotropic hole mass as $m_h=0.195m_0$ by Skolnick and Bimberg.[17]

The phonon of $2H$-polytype PbI_2 has been extensively studied. The optical-phonon energies of the E_g and A_{1g} modes are 75 and 97 cm^{-1}, respectively.[18] In the acoustic-energy region of the Raman spectrum, there appears a shear mode which is one of the rigid-layer modes and has an energy characteristic of the polytype.[19] The energy dispersions obtained by Sears, Klein, and Morrison[20] are in good agreement with dispersion spectra obtained from inelastic neutron scattering.[21] However, the compressional mode, which is the other rigid-layer mode, is Raman inactive.

In an ultrathin crystal, however, the rigid-layer mode has not been studied yet, to our knowledge. The optical properties in the visible region of a PbI_2 ultrathin film have been investigated by some groups[7] and in our laboratory,[8,9] but estimations of the film thickness were not very clear.

We have prepared PbI_2 ultrathin microcrystallites with various thicknesses in the organic polymer ethylene metacrylic acid (E-MAA) supplied from Mitsui du Pont Polychemical Co. A Raman line characteristic of the layer number appears in the resonant Raman spectrum and is analyzed using a finite-linear-chain model. From analysis of the Raman spectra, the layer number of the ultrathin microcrystallites is estimated, and using this

0163-1829/95/52(8)/5929(6)/$06.00

layer number the quantum confinement of the exciton translation motion is discussed.

II. EXPERIMENT

Microcrystallites of PbI_2 were prepared by exchange of a hydrogen ion of E-MAA copolymer for a Pb^{2+} ion, followed by a reaction with HI gas. The thickness of the crystallites was controlled by heat treatment of the stretched polymer film. The details were already reported in the previous paper.[9]

From measurement using a transmission electron microscope (TEM), the PbI_2 microcrystallite is known to be platelet shaped.[9] The lateral diameter ranges from 2 to 80 nm, depending on the thickness.

For measurement of the absorption spectrum, the polymer film containing PbI_2 microcrystallites was immersed into pumped liquid helium. Transmitted light was detected using a system of an incandescent lamp, a double monochromator, a photomultiplier tube, and a picoammeter in the visible region, and of a deuterium lamp, a single monochromator, and a multichannel detector in the ultraviolet region.

The measurements of Raman scattering spectra were carried out at liquid-nitrogen temperature. A dye laser pumped by Ar^+ laser light was used as a light source. The active medium of the dye laser was Stilben 420 and Coumarin 480, for which the tuning range was between 2.5 and 2.9 eV. The intensity of the excitation laser light on the surface of the sample was less than 1 W/cm^2. Backscattered light from the irradiated surface was guided into a Jobin-Yvon U-1000 double monochromator and detected with a Hamamatsu Photonics R-636 photomultiplier tube. The full width at half maximum (FWHM) of this system was less than 1 cm^{-1}.

III. RESULTS AND DISCUSSION

From the measurements of electron-beam scattering in microcrystallites with several layers, the lattice constant and the crystal symmetry are known to be almost the same as those of the bulk. Accordingly, the layer thickness is considered to be about 0.7 nm even in the ultrathin microcrystallites.

Figure 1 shows absorption spectra of samples with various heat treatments at 2 K. The sample number of each spectrum is shown on the right-hand side. There appear five structures at 2.5–2.8 eV (A), 3.1 eV (E), 3.4–3.5 eV (B), 3.8–4.2 eV (C), and 4.5–4.6 eV. The average thickness of the microcrystallites increases in order from the lowest spectrum. Within structure A, the main peak energy shifts to lower energies in order from the lowest curve, and the peak energies of bands B and C show the same behavior. The energies of these bands in the uppermost curve are close to those of the bulk crystal. From the correspondence with the bulk, structure A is considered to be due to exciton formation associated with an $A_4^+ \rightarrow A_4^-$ interband transition, as reported previously.[12] Bands B and C correspond to the bulk exciton transitions $A_4^+ \rightarrow A_{5,6}^-$ and $A_4^+ \rightarrow A_4^-$, respectively.[12] The existence of the three bands suggests that the same

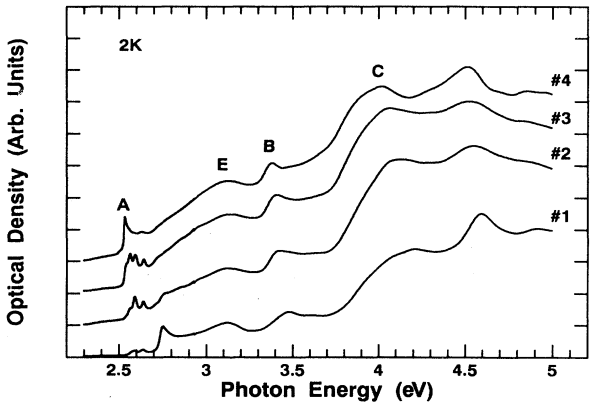

FIG. 1. Absorption spectra of PbI_2 microcrystallites in E-MAA copolymer with various heat treatments at 2 K.

electronic transitions occur in the microcrystallite as in the bulk.

The energy shifts of these absorption bands from the bulk are different. This may be caused by the difference in the effective electron mass in the corresponding conduction bands.

On the other hand, band E is considered to be due to a dipole transition between the lowest conduction and the highest valence bands at general points of the Brillouin zone. This band energy is independent of the crystal thickness, which is reasonable because the E band reflects the density of states in the entire Brillouin zone. In addition, the band at around 4.5 eV is assigned as a transition from the next deeper valence band to the lowest conduction band, by the analogy with the bulk crystal.[12]

Figure 2 shows detailed absorption spectra around structure A. Letters in this figure are explained later. As the crystal thickness increases, the highest-energy band disappears and new absorption band appear on the lower-energy side. These bands are considered to be due to the exciton confined in the direction of the c axis of the microcrystallites, as reported previously.[9]

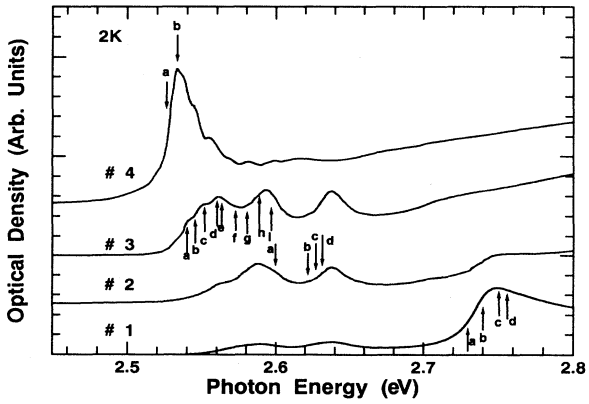

FIG. 2. Expanded spectra of Fig. 1 around the structure A. Letters and arrows show excitation energies of the resonant Raman spectra in Figs. 3 and 4.

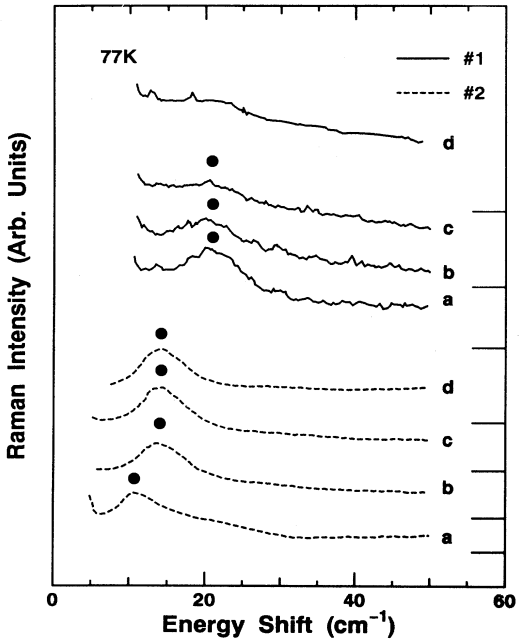

FIG. 3. Raman spectra of samples 1 and 2 in the excitations with various energies at 77 K. Solid and dotted curves are resonant Raman spectra of samples 1 and 2, respectively. Excitation energies are show by letters in Fig. 2. Peak energies are marked by closed circles.

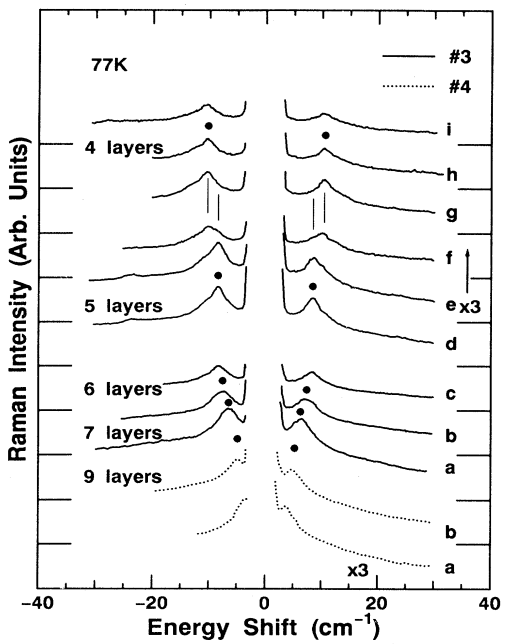

FIG. 4. Raman spectra of samples 3 and 4 at 77 K. The lowest two lines are Raman spectra of sample 4 and the others are 3. On the left-hand side is shown the layer number of the crystallite which is excited by light with the exciton peak energy. Excitation energies are shown in Fig. 2.

To begin with, we study phonon properties in the ultrathin crystallite, because clear information about the crystal thickness is also obtained from this study.

Figures 3 and 4 show the Raman spectra of some polymers containing microscrystallites with various thicknesses under the excitation of laser light with different energies at 77 K. The excitation energies are shown by arrows and letters in Fig. 2. The peak energies of the absorption spectra at 77 K are almost the same as those at 2 K but the fine structures disappear due to phonon broadening. The solid and broken curves in Fig. 3 are Raman spectra of samples 1 and 2, respectively. In Fig. 4, the lowest two curves are measured using sample 4 and the others using sample 3. The excitation energy increases in order from the lowest curve in Figs. 3 and 4. The layer number in Fig. 4 shows that the excitation energy coincides with the corresponding exciton absorption band. These layer numbers are determined in the following discussion. Stokes and anti-Stoke shifts of the Raman lines marked with dots in Figs. 3 and 4 become larger as the excitation energy increases. Since no structure is observed in this energy region of the Raman scattering spectrum in Pb^{2+}-doped polymer without PbI_2 microcrystallites, these structures are not associated with the polymer. If the Raman line is associated with any phonon of the bulk crystal, the energy shift should be independent of the excitation energy. However, this is not the case. Hence, it appears that this line is caused by a phonon of the PbI_2 microcrystallite.

Here, we discuss the origin of this line. It has the following characteristics. First, the Stokes and anti-Stokes shifts are independent of the inhomogeneous width of the absorption bands. The absorption bandwidth is considered to be related to the lateral size distribution.[22] For example, broken curves *b*, *c*, and *d* of sample 2 in Fig. 3 are Raman spectra in the excitation energies corresponding to the energy level of the exciton confined in a microcrystallite with the given layer numbers, as shown in Fig. 2. The Raman lines for these three spectra show the same Stokes shift in spite of the different excitation energies. Secondly, the Stokes shifts of the Raman lines in the lowest curve *a* of Fig. 3 and curve *i* of Fig. 4 for nearly the same excitation energies are the same, although samples of these two spectra have different size distributions. Thirdly, the Stokes and anti-Stokes shifts of the Raman line are characteristic of the layer numbers. For example, the excitation energies of spectra *e*, *f*, and *g* in Fig. 4 are located between the two exciton bands at 2.559 and 2.590 eV of sample 3 as shown in Fig. 2, where two Raman lines are observed. These may correspond to phonons generated in two kinds of the microscrystallites with different layer numbers. From these characteristics, the observed Raman line is concluded to be associated with a phonon, the energy of which depends on the layer number of the microcrystallite.

It is known that a Raman line appearing in this energy region of the bulk is associated with a rigid-layer phonon which exists in the polytypes except $2H$.[20] In layered semiconductors, the interlayer bonding is much weaker than the intralayer one. Hence, a rigid layer mode ap-

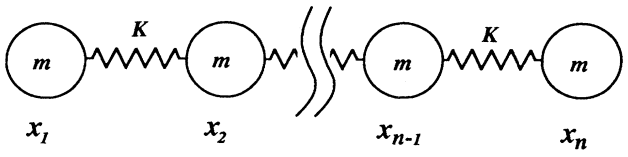

FIG. 5. Schematic diagram of the linear-chain model. The letter m means the mass of the unit layer, K the force constant, and x_i the displacement of the ith layer ($i=1,2,3,\ldots,n$).

pears in the low-frequency region of the Raman scattering spectrum. In the bulk crystal, it is assumed that the boundary condition is periodic.[20] In the ultrathin microcrystallite, however, the crystal boundary should be assumed to be free. If the polymer matrix surrounding the microcrystallites plays an important role in the vibration, the observed Raman line should be broadened. However, this is not the case. Moreover, the elastic constant of the polymer is about ten times as weak as that of PbI_2 in the c direction. Therefore the effect of the matrix on the vibration energy of the microcrystallite may be neglected.

Here, we propose a linear-chain model in interpret the observed Raman spectrum. Figure 5 shows a schematic diagram in which the n rigid layers are represented by mass m and are bonded with each other by a force constant K. Displacements of the ith layer ($i=1,2,3,\ldots,n$) are expressed by x_i. The equations of the layer motions are written as

$$m\frac{d^2x_1}{dt^2}=-K(x_1-x_2)\,, \tag{1}$$

$$m\frac{d^2x_2}{dt^2}=-K(x_2-x_1)-K(x_2-x_3)\,, \tag{2}$$

$$\vdots$$

$$m\frac{d^2x_{n-1}}{dt^2}=-K(x_{n-1}-x_{n-2})-K(x_{n-1}-x_n)\,, \tag{3}$$

$$m\frac{d^2x_n}{dt^2}=-K(x_n-x_{n-1})\,, \tag{4}$$

i.e.,

$$m\frac{d^2}{dt^2}\begin{pmatrix}x_1\\x_2\\\vdots\\x_{n-1}\\x_n\end{pmatrix}=-K\begin{pmatrix}1&-1&0&\cdots&0&0&0\\-1&2&-1&\cdots&0&0&0\\\vdots&\vdots&\vdots&\ddots&\vdots&\vdots&\vdots\\0&0&0&\cdots&-1&2&-1\\0&0&0&\cdots&0&-1&1\end{pmatrix}\begin{pmatrix}x_1\\x_2\\\vdots\\x_{n-1}\\x_n\end{pmatrix}. \tag{5}$$

We can choose two kinds of force constants: one is the force constant of a shear mode K_s and the other that of a compressional mode K_c. The phonon energies calculated from Eq. (5) using the parameters $K_c=7.0$ N/m, $K_s=1.67$ N/m,[20] and $m=1.660\times10^{-27}$ kg in the bulk are shown by open symbols in Fig. 6. Open circles and triangles represent the energies of the compressional and shear modes, respectively. Here, the phonon of the longest wavelength is selected, because the interaction between the shorter-wavelength phonon and the confined excitation may be weaker. The reason for this is given later.

Experimental phonon energies are plotted with closed circles as a function of the layer number in Fig. 6 on the assumption that the phonon energy coincides with that of the Raman shift. The thickness is represented by L on the abscissa. Here, the layer numbers are determined such that the Raman shift is equal to the calculated energy of the compressional-mode phonon with the longest wavelength, as shown by open circles. This good correspondence between the open and closed circles suggests that the confined exciton interacts with the compressional mode and that the exciton band at the highest energy 2.75 eV is associated with the microcrystallite having two layers.

Raman scattering of bulk PbI_2 is forbidden for the compressional mode but allowed for the shear mode from group analysis.[19] In this experiment, however, the excitation energy is resonant with the exciton energy. Furthermore, PbI_2 microcrystallites have symmetry different from that of the bulk crystal because of the finite layers. Hence the selection rule for Raman scattering of the bulk cannot be applied.

Let us consider the reasons why the compressional-mode phonon with the longest wavelength couples with the spatially confined exciton. The vibrational direction for the compressional mode is the same as that of the exciton confinement. Both the spatially confined exciton and the deformation potential induced by the lowest-energy phonon are expressed by a standing wave with the same length $2L$ and phase. Therefore a deformation-potential-type interaction may be strong. On the other hand, the higher-energy phonons have wavelength smaller than that of the exciton, and hence the interaction with the exciton may become weaker.

Next, we will discuss the excitation energy of the microcrystallites. Figure 7 shows exciton absorption spectra of different samples in the energy region between 2.5 and 2.8 eV at 2 K, which are the same spectra as in Fig. 2. The number near each absorption band indicates the layer number of the PbI_2 microcrystallite in which the exciton corresponding to the band is confined. These layer numbers are determined from the phonon assignment mentioned above, and are different from those of our pre-

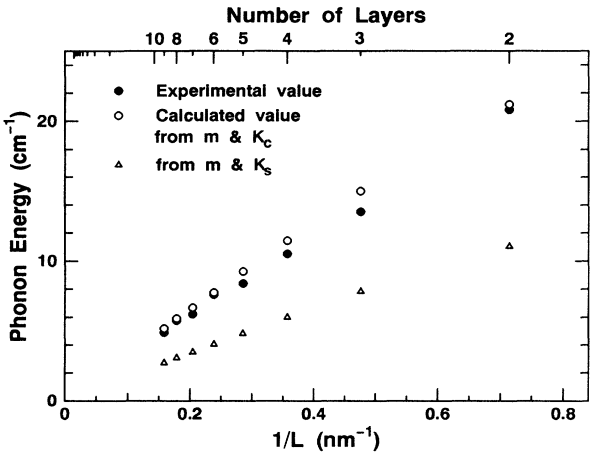

FIG. 6. The calculated and experimental phonon energies are shown as a function of $1/L$, where L is the crystal thickness and equals half the wavelength of the phonon. Open circles and triangles show phonon energies calculated using the force constants for the compressional and shear modes, respectively, of the bulk phonons. Closed circles show the measured phonon energies.

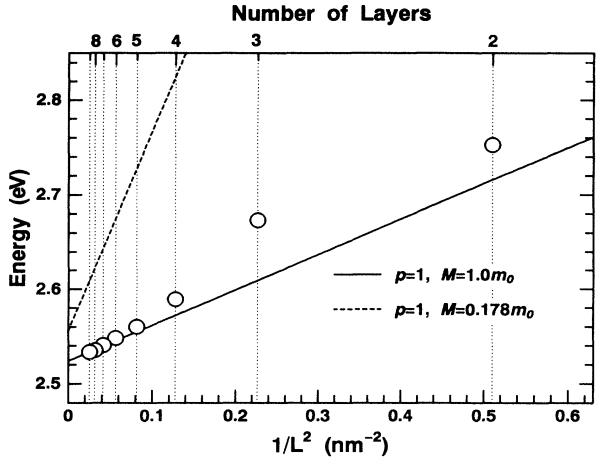

FIG. 8. Peak energies of the absorption bands in Fig. 7 are shown by open circles as a function of $1/L^2$. Layer numbers corresponding to the crystal thickness are indicated on the upper abscissa. The solid line represents the calculated linear relation E vs $1/L^2$ of Eq. (6). The broken line represents the calculated relation on the basis of the electron-hole confinement model.

vious paper.[9]

Both the peak energy and the width of the exciton absorption band increase as the thickness of the microcrystallite becomes smaller. Here, we consider that the exciton translational motion is spatially confined in the direction of the c axis, as assigned previously.[9] These discrete absorption bands correspond to the discrete thickness which are caused by the finite layers. The peak energies of the exciton bands are plotted as a function of $1/L^2$ in Fig. 8. If the exciton is confined within the infinite potential well at the crystal boundary in the direction of the c axis, the exciton energy E in an effective-mass approximation is expressed by

$$E = E_B + \frac{\hbar^2}{2M}\frac{\pi^2 p^2}{L^2}, \tag{6}$$

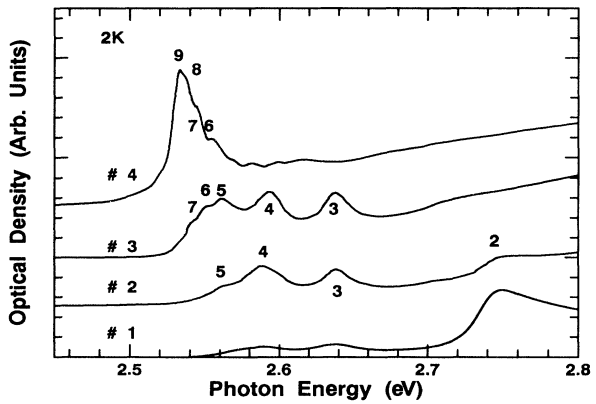

FIG. 7. The same absorption spectra as in Fig. 2. The numbers on the absorption bands how layer numbers of the PbI_2 microcrystallites where the corresponding excitations are confined.

where E_B is the exciton formation energy in the bulk and M the exciton translation mass, L the width of the potential well, and p the quantum number of the confinement corresponding to the number of loops of the standing wave.

The solid line in Fig. 8 represents Eq. (6) with $M = 1.0m_0$, $E_B = 2.524$ eV, and $p = 1$, where m_0 is the free-electron mass. This M is equal to the exciton total mass in the direction of the c axis of the $4H$-type single crystal,[15] and the value of E_B is cited from Tubb's paper.[10]

On the other hand, the broken line represents Eq. (6) with the isotropic reduced mass $M = 0.178m_0$,[16,17] under the electron-hole individual confinement model, where E_B is the formation energy of the electron-hole pair. The solid line shows a good fit to the experimental peak energies, as shown by open circles, in the range of the abscissa less than 0.1. This coincidence strongly suggests that the translational motion of the exciton is quantized in crystallites with more than five layers.

In contrast, the exciton energies in the two- and three-layer crystallites are much higher than those given by the solid line. This deviation may be caused mainly by transfer from "exciton confinement" to "electron-hole confinement." This may be intimately related to the ratio of the effective Bohr radius of the A exciton, 1.9 nm,[14] to the potential well width, as pointed out by Kayanuma.[23]

IV. CONCLUSION

In the resonant Raman spectra of PbI_2 microcrystallites in polymer, a new Raman line is observed in the low-energy region. This Raman line is considered to be due to the compressional-mode phonon. The relationship

between the Raman shift and the layer thickness corresponding to the resonant excitation is well described by a linear-chain model. From this relation, we obtain the correspondence between the exciton absorption band and the layer number, which shows that the layer number determined previously should be changed. The reinterpretation of the A-exciton energy in the ultrathin crystallite leads to the conclusion that the energy shift of the exciton confined in crystallites with more than five layers is well explained by an effective-mass approximation. However, the exciton energies in thinner crystallites deviate from the theoretical value. This discrepancy may be mainly caused by transfer from exciton confinement to electron-hole confinement.

ACKNOWLEDGMENTS

The authors would like to thank Professor Sasaki, Ishinomaki Senshu University, and Professor Ekimov, Ioffe Physical Technical Institute, Russia, for helpful discussions. They also thank M. Saito, Tohoku University, for technical assistance. This work was supported by a Grant-in-Aid for Scientific Research from the Ministry of Education, Science and Culture of Japan.

*Present address: Institute for Solid State Physics, University of Tokyo, Tokyo 106, Japan.

[1]For example, see recent reviews and references in A. D. Yoffe, Adv. Phys. **42**, 173 (1993).

[2]J. Kusano, Y. Segawa, M. Mihara, Y. Aoyagi, and S. Namba, Solid State Commun. **72**, 215 (1989).

[3]A. D'Andrea, R. Del Sole, and K. Cho, Europhys. Lett. **11**, 169 (1990); H. Tuffigo, B. Lavigen, R. T. Cox, G. Lentz, N. Magnea, and H. Mariette, Surf. Sci. **229**, 480 (1990); A. Tredicucci, Y. Chen, F. Bassani, J. Massies, C. Deparis, and G. Neu, Phys. Rev. B **47**, 10 348 (1993).

[4]Z. K. Tang, A. Yanase, T. Yasui, and Y. Segawa, Phys. Rev. Lett. **71**, 1431 (1993).

[5]R. F. Frindt, J. Appl. Phys. **37**, 1928 (1966); B. L. Evans and P. A. Young, Proc. Phys. Soc. London **91**, 475 (1967).

[6]F. Consandori and R. F. Frindt, Phys. Rev. B **2**, 4893 (1970).

[7]V. K. Miloslavskii, A. I. Rybalka, and L. A. Agreev, Fiz. Tverd. Tela (Leningrad) **17**, 1150 (1975) [Sov. Phys. Solid State **17**, 733 (1975)]; V. V. Mussil, V. K. Miloslavskily, A. I. Rybalka, and Ngen Van Tien, Solid State Commun. **17**, 1025 (1975); C. J. Sandroff, S. P. Kelty, and M. Hwang, J. Chem. Phys. **85**, 5337 (1986); E. P. Pokatilov, S. I. Beril, V. M. Fomin, V. G. Litovchenko, D. V. Korbutyak, E. G. Lashekevich, and E. V. Mikhailovskaya, Phys. Status Solidi B **145**, 535 (1988).

[8]T. Goto and Y. Sasaki, J. Phys. Soc. Jpn. **53**, 4432 (1984); T. Goto and J. Maeda, *ibid.* **56**, 3710 (1987).

[9]T. Goto, S. Saito, and M. Tanaka, Solid State Commun. **80**, 331 (1991).

[10]M. R. Tubbs, J. Phys. Chem. Solids **29**, 1191 (1968).

[11]E. Doni, G. Grosso, and G. Spavieri, Solid State Commun. **11**, 493 (1972).

[12]I. Ch. Schlüter and M. Schlüter, Phys. Rev. B **9**, 1652 (1974).

[13]J. Bordas, J. Robertson, and A. Jakobsson, J. Phys. C **11**, 2607 (1978).

[14]Y. Nagamune, S. Takeyama, and N. Miura, Phys. Rev. B **40**, 8099 (1989).

[15]T. Hayashi, J. Phys. Soc. Jpn. **55**, 2043 (1986).

[16]T. Goto, J. Phys. Soc. Jpn. **51**, 3 (1982).

[17]M. S. Skolnick and D. Bimberg, Phys. Rev. B **18**, 7080 (1978).

[18]S. Nakashima, Solid State Commun. **16**, 1059 (1975); R. Zallen and M. L. Slade, *ibid.* **17**, 1561 (1975).

[19]R. Loudon, Adv. Phys. **13**, 423 (1964).

[20]W. M. Sears, M. L. Klein, and J. A. Morrison, Phys. Rev. B **19**, 2305 (1979).

[21]B. Dorner, R. E. Ghosh, and G. Herbeke, Phys. Status Solidi B **73**, 655 (1976).

[22]T. Goto and S. Saito, in *Quantum Well and Superlattice Physics IV,* edited by G. H. Doehler, SPIE Proc. Vol. 1675 (SPIE, Bellingham, WA, 1992), p. 128.

[23]Y. Kayanuma, Phys. Rev. B **38**, 9797 (1988).